Quenching Control and Distortion, September 9–13, 2012, Chicago, Illinois, USA
Proceedings from the 6th International Quencing and Control of Distortion Conference
Including the 4th International Distortion Engineering Conference
D. Scott MacKenzie, editor



# Heat Transfer Coefficients during Quenching of Inconel and AISI 304 Stainless Steel Cylinders in $NaNO_2$ Aqueous Solutions

D.E. Lozano[1] , R.D. Mercado-Solís[1] , R. Colás[1], L.F. Canale[2], G.E. Totten[3]

1. Universidad Autónoma de Nuevo León, San Nicolás de los Garza Nuevo León, México
2. Universidade de Sao Paulo, Sao Carlos, SP, Brasil
3. Portland State University; Portland, Ore., USA

**Keywords:** Heat transfer coefficient, quenching, sodium nitrite

## Abstract

In order to reduce distortion and cracking when quenching in water, uniform cooling must be promoted while avoiding full-film boiling. The formation of a vapor blanket may be prevented either by imposing severe agitation or by quenching in aqueous salt solutions. Furthermore, with the addition of the optimum salt concentrations, the cooling rate may be favorably increased. In this work, the cooling characteristics of round-bars of Inconel (ø12.6 mm) and AISI 304 stainless steel (8, 12 and 20 mm in diameter) heated to 900°C and quenched by immersion into aqueous solutions of 2, 3, 4 and 9% sodium nitrite ($NaNO_2$) were studied. Time-temperature cooling curves were obtained using embedded thermocouples within the probes and the heat transfer coefficients and cooling rates were calculated. It was found that an increase of $NaNO_2$ concentration beyond 4% did not result in a corresponding increase in the cooling ability of the quenchant.

## Introduction

Brine (NaCl) and caustic (NaOH) quenchants are the most common salts added to water for quenching when it is desired to accelerate the cooling process. At optimum concentrations, these salts not only increase the heat extraction capacity but provide more uniform cooling by destabilizing the vapour blanket and reducing the film-boiling stage, which is a low heat transfer stage [1]. Since high cooling rates are obtained by using these quenchants, its use is usually limited to low hardenability steels due to crack and distortion propensity and because these salts are typically corrosive to steels.

On the other hand, sodium nitrite ($NaNO_2$) has been used as an additive in quenching processes for different purposes. For instance, in molten salt bath quenching, it is used for cooling rate control [2,3]. Sodium Nitrite is also added as a corrosion inhibitor to many aqueous polymer quenchants [4,5].

Kobasko [6] states that decreasing or eliminating the full-film boiling, which often leads to non-uniform cooling and by increasing the cooling rate up to values greater than 600°C/s, the probability of cracking and distortion is minimized. Intensive quenching processes may utilize sodium nitrite as a corrosion inhibitor in highly agitated aqueous solutions [7]. The high cooling rates attained in this process are due to severe agitation and high mass flow rates in addition to the use of salt solutions such as aqueous sodium nitrite which acts like a brine quenchant.

Although the use of sodium nitrite is widely employed, the effect of the $NaNO_2$ addition in the cooling power of water has not been addressed in literature. The present work studies the cooling capacity of $NaNO_2$ aqueous solutions at different concentrations.

**Heat Transfer and Heat Flux Density Determination**

Heat Transfer Coefficient (HTC) and Heat Flux Density are commonly calculated after surface temperature determination. The following equations are used:

$$\dot{q} = -\lambda \frac{\Delta T}{\Delta x} \quad (1)$$

$$\alpha = \frac{\dot{q}_{surface}}{T_{surf.} - T_{quenchant}} \quad (2)$$

where $\dot{q}$ is the heat flux density, $\lambda$ thermal conductivity (temperature dependent), $\Delta T$ is the difference between surface temperature and an inner node temperature, $\Delta x$ is the distance between the two points and $\alpha$ is the HTC.

The surface temperature is obtained by the usage of a parabolic temperature distribution described in Reference [8]. This method requires the use of three thermal histories and then the surface temperature is calculated solving the second order equation of a parabola as follows:

$$\begin{vmatrix} a(x_1 - n)^2 & b(x_1 - n) & c \\ a(x_2 - n)^2 & b(x_2 - n) & c \\ a(x_3 - n)^2 & b(x_3 - n) & c \end{vmatrix} = \begin{matrix} T_1(t) \\ T_2(t) \\ T_3(t) \end{matrix} \quad (3)$$

where,
$x_1 =$ (distance from surface to the innermost thermocouple),
$x_2 =$ (distance from the surface to the intermediate thermocouple),
$x_3$(distance from the surface to the outermost thermocuple, as near to the surface as possible, 1mm)
n=distance from surface to the point of interest Tn.

For the surface temperature, the boundary conditions are: (n=0), ($T_{surface} = T_n = c$);
$n = x_n = 0$, therefore $T_n(t) = c$, then solving the matrix, the constant "c" is obtained as a function of time,$T_1$, $T_2$ and $T_3$.

## Experimental

A standard INCONEL 600 probe according the ASTM D-6200 [9] was used to obtain the cooling curves of the aqueous solutions (see Figure 1). This type of cylindrical probe (Ø12.5 mm x 60 mm) uses a single thermocouple located at the geometric center and is useful for determination of the cooling characteristics of quenchants for comparison. However for an accurate heat transfer determination, the temperature near the surface must be known.

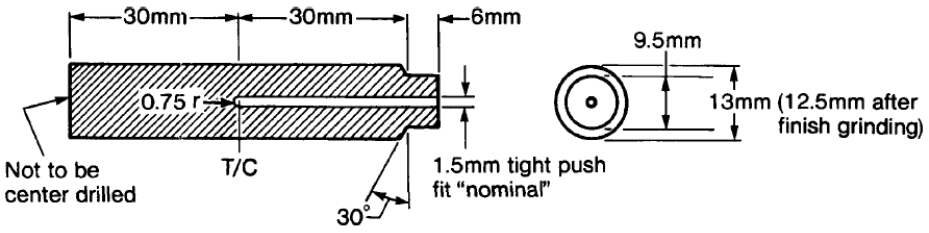


*Figure 1 Geometry of the standard INCONEL 600 probe* [9]

It is commonly assumed that a diameter/length ratio of at least (1:4) will adequately minimize end cooling effects and then the heat transfer calculation can be treated as a one-dimensional (1D) problem which simplifies the computations. Therefore, cylindrical probes of three diameters (8, 12 and 20 mm) of an AISI 304 austenitic stainless steel were fabricated. The probe length was 5 times greater than their diameters (40, 60 and 100mm respectively). Three Ø1mm blind holes were drilled by electro discharge machining up to the mid length in each of the probes. The holes were drilled at the center, mid-radius and at 1 mm from the surface in each probe. In Figure 2, a schematic illustration for the Ø12 mm probe is shown. The dimensional relationships shown in this figure is valid for the Ø8 and Ø20 mm probes also.

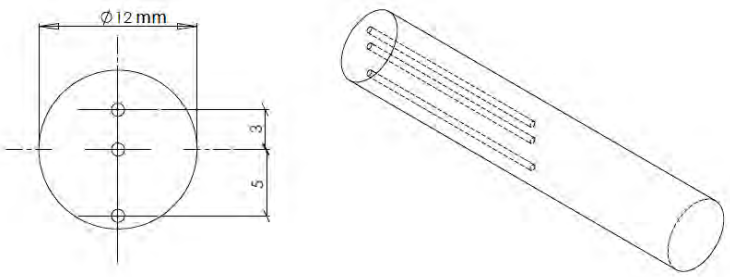


*Figure 2 Geometry of the Ø12 mm and 60mm length AISI 304 austenitic stainless steel probe, showing thermocouple positions.*

Three ungrounded Ø1 mm Type-K thermocouples were inserted into the holes. The holes were machined in order to tightly adjust the thermocouples. A small amount of graphite powder was deposited into the holes before thermocouple insertion to ensure good contact between the thermocouple and the probe and to fix the thermocouple. After thermocouple placement, a ceramic coating was used to seal the holes to prevent the quenchant from entering the holes.

The thermocouples were differentially connected (negatives were connected to different channels not to ground) using a 75 KΩ resistor between the negative terminal and ground to have a good reference. Data was acquired at 100 Hz frequency and was averaged to 10 points per second for the cooling rate and heat transfer calculations.

Probes were heated to 900°C and then quenched. A glass reservoir, 200 mm diameter and 500 mm high, with 12 liters of quenchant was used. All experiments were performed at quenchant temperature of 25-27 °C. The temperature of the quenchant was measured. A localized quenchant temperature increase (from 25 to 45°C ) was recorded in the upper zones of the liquid near surface. After each experiment the quenchant was mixed and no considerable temperature increase was measured (≈1 to 2 °C).

## Results and Discussion

Figure 3 shows the cooling time-temperature curves (a) and the cooling rate curves (b) for tap water, and aqueous 2, 3, 4 and 9 % $NaNO_2$ solutions obtained using the standard INCONEL 600 probe. It can be seen (Fig. 3a) that increasing the $NaNO_2$ concentration produces a proportional reduction of the film-boiling duration up to 4%. It was noted that the 4% and 9% cooling curves overlapped. Figure 3b shows that the cooling rate was 2.1 times greater with 4% $NaNO_2$ addition than that obtained under the same conditions for water.

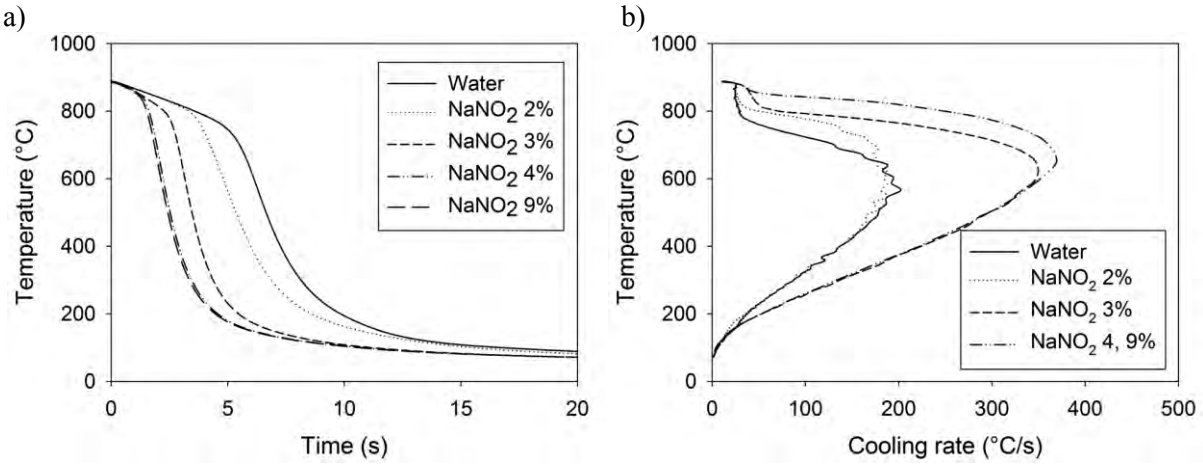


*Figure 3 Cooling curves of a Ø12.5 mm INCONEL 600 probe (a) and cooling rate curves (b).*

Figure 4 shows the experimentally obtained cooling curves of the Ø12 mm stainless steel probe and its calculated surface temperature for tap water (a) and for 4 % $NaNO_2$ (b). During water quenching, duration of the film-boiling stage is 3 seconds (780°C) while the duration of the film boiling stage for the $NaNO_2$ solution is considerably reduced or even eliminated.

Figure 5 shows the heat flux density as function of time for both cases. The heat flux density was calculated using the calculated surface temperature and also the calculated temperature 0.1 mm below surface. Figure 5a shows three stages of quenching, from left to right, full-film boiling , nucleate boiling and convection. The first and second critical flux densities are illustrated. In Figure 5b, only nucleate boiling and convection are noticeable. The increase in the heat flux density during the nucleate boiling was almost 3 times greater that obtained for the aqueous $NaNO_2$ solution (6 $MW/m^2$).

Figure 6 shows the effect of the $NaNO_2$ addition on the heat transfer coefficient. The HTC for tap water was 10 $KW/m^2$ K which is in good agreement with the value found for water according to Narazaki [10], whose experiments were conducted using a Ø10 mm silver probe. A direct comparison cannot be made because the diameter and material difference. The HTC for the 4 % solution reached a maximum of 45 $KW/m^2$ K. This value is similar with the 42-47 $KW/m^2$ K reported by Narazaki for 10% brine (NaCl). Once again, for a direct comparison, the size and material of the probe must be considered. Kobasko [1,6] reported values of the average effective HTC of 16 $KW/m^2$ K for 10 % brine, however this lower value may be derived by the method of HTC determination. If the thermal history at the center of the probe of experiment of Figure 4b is used to calculate the average effective HTC via the method described in ref. [11] and [12], a value of 9 $KW/m^2$ K is obtained.

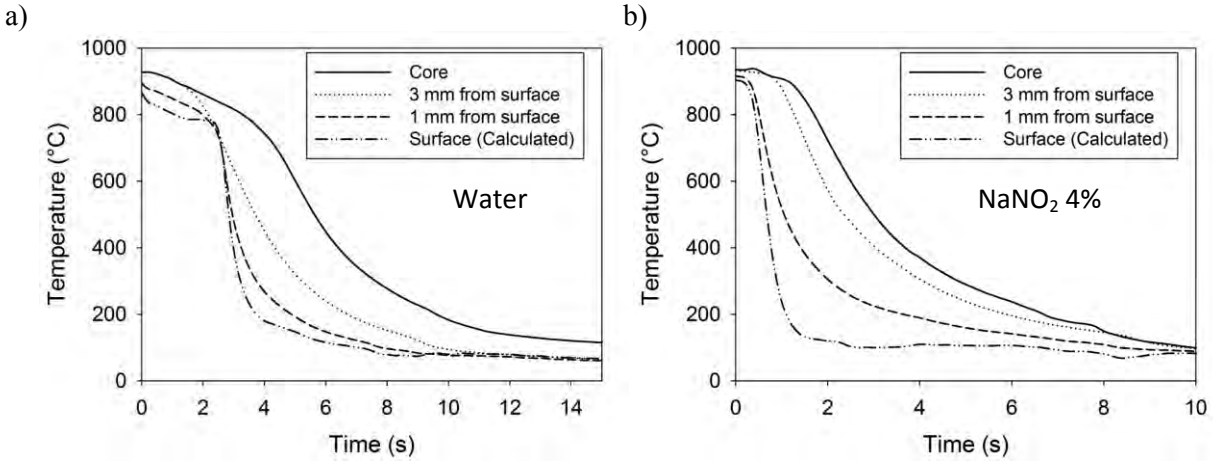


*Figure 4 Cooling curves of a Ø12 mm AISI 304 stainless steel probe quenched in tap water (a) and $NaNO_2$ 4% aqueous solution (b)*

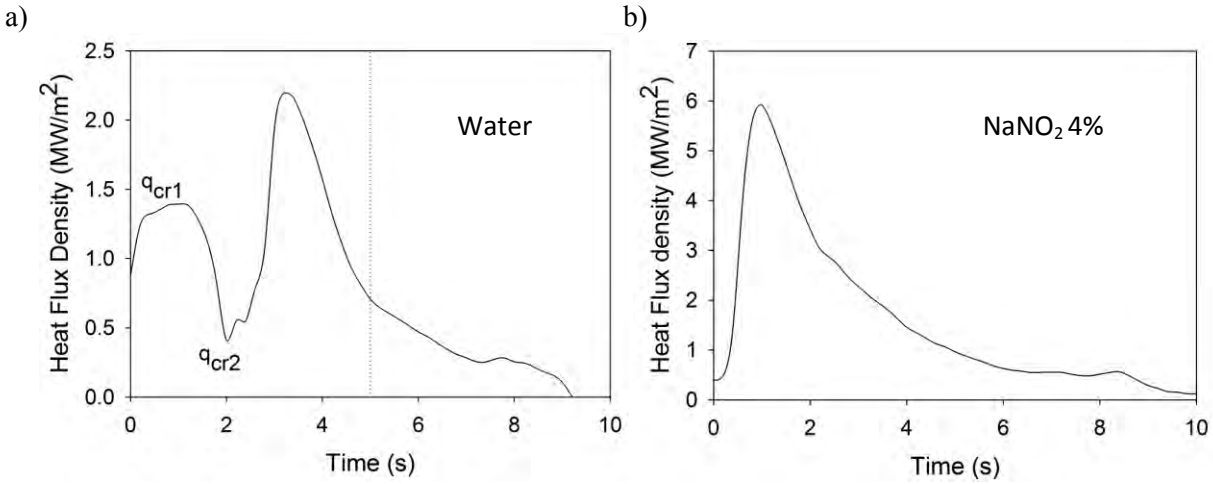


*Figure 5 Heat Flux density as function of time for water (a) and $NaNO_2$ 4% aqueous solution (b)*

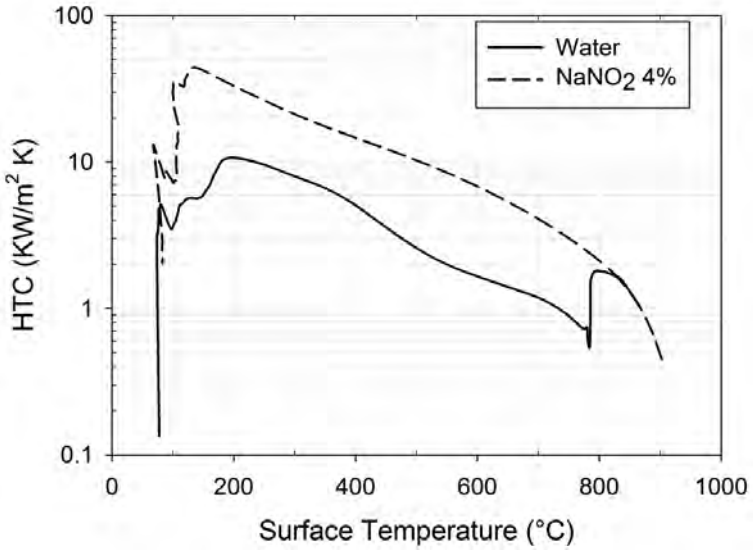


*Figure 6 HTC as function of surface temperature of Ø12 mm AISI 304 stainless steel probe*

Experiments using 8 and 20 mm diameter probes were also performed in order to analyze the effect of probe size on the HTC and on the heat flux density (Figure 7 and 8 respectively). As expected, an increase in the diameter corresponds to a reduction of the HTC and heat flux. According to the heat flux as function of time figure, a linear correlation was found between the HTC and the diameter (Figure 9). However, it is important to point out that this linear relationship could be non-linear for greater diameters as Liscic reported in Reference [13] and concluded that no simple correlation can be determined as function of diameter.

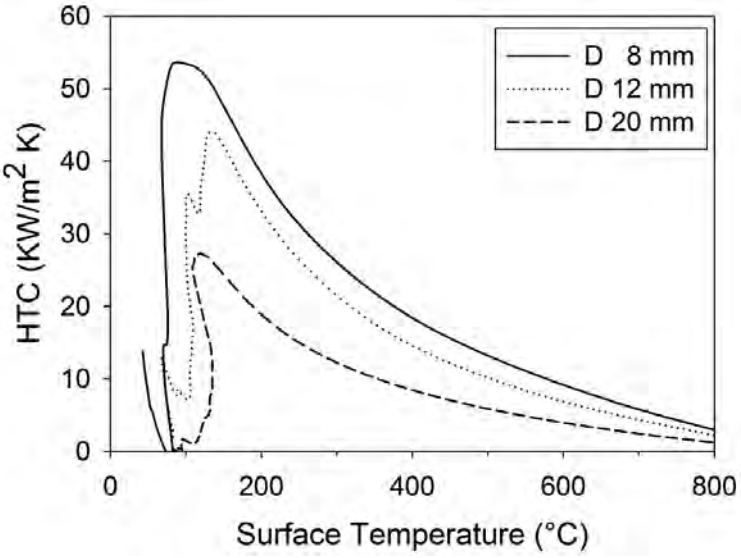


*Figure 7. HTC as function of surface temperature of AISI 304 stainless steel probes with different diameters when quenched in $NaNO_2$ 4% aqueous solution*

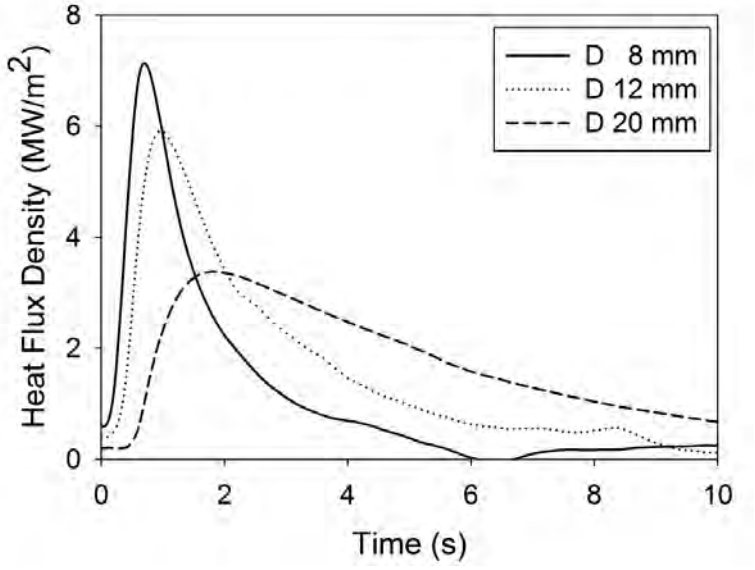


*Figure 8. Heat flux density as function of time of AISI 304 stainless steel probes with different diameters when quenched in $NaNO_2$ 4% aqueous solution*

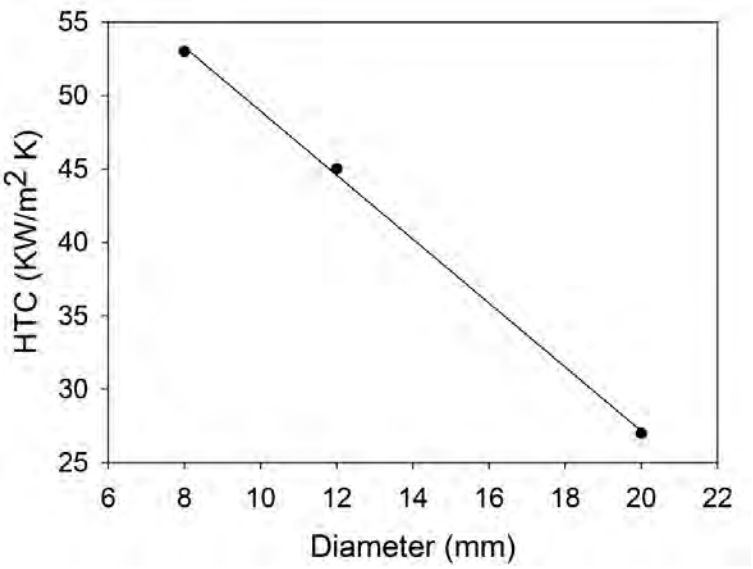


*Figure 9 HTC as function of bar diameter*

## Conclusions

The effect of $NaNO_2$ addition to water on the cooling mechanism was evaluated. It was found that the optimal concentration at which the maximum cooling rates are obtained is 4%, and further additions do not increase the cooling capacity of the quenchant. The HTC obtained with this 4% concentration was similar to the HTC obtained by Narazaki [10] for 10% brine. The full-film boiling stage was prevented and therefore more uniform cooling could be expected.
A linear correlation was foud for the evaluation of HTC for different probe diameters. However this correlation could be non-linear for greater diameters according to some authors [12]. Further research to determine a valid correlation for a wider range of probe dimeters and quenchants is suggested.

## Acknowledgments

The authors thank Consejo Nacional de Ciencia y Tecnología (CONACYT-México), Universidad Autónoma de Nuevo León and Facultad de Ingeniería Mecánica y Eléctrica for their financial support.

## References

[1] G.E. Totten, C.E. Bates and N.A. Clinton, Other Quenching Processes, Handbook of Quenchants and Quenching Technology, ASM International, 1993, p 304-309.

[2] F.R. Morral, Quenching Steel in Molten Salts, Steels, p 92-116.

[3] G.P. Dubal, Salt Bath Quenching, Advanced Materials & Preocesses, Vol. 156, No. 6, 1999,p H23-H28.

[4] G.E. Totten, C.E. Bates and N.A. Clinton, Other Quenching Processes, Handbook of Quenchants and Quenching Technology, ASM International, 1993, p 161-190.

[5] M. Cohen, Inhibition of Steel Corrosion by Sodium Nitrite in Water, Journal of The Electrochemical Society, Vol 93 No. 1, 1948.

[6] N.I. Kobasko, M.A. Aronov, J.A. Powell & G.E. Totten,Intensive Quenching Systems: Engineering and Design, ASTM 2010.

[7] M.A. Aronov, N.I. Kobasko & J.A. Powell, Applications of Intensive Processes for Carburized Parts, 2nd Int. Surf. Eng. Cong., 2003, p 169-173.

[8] D.E. Lozano, R.D. Mercado-Solis, R. Colas, L.F. Canale & G.E. Totten, Surface Temperature and Heat Transfer Coefficient Determination during Quenching, QCD Conference, Currently in review.

[9] ASTM D6200-01, Standard Test Method for Determination of Cooling Characteristics of Quench Oils by Cooling Curve Analysis, ASTM Int., 2007.

[10] M. Narazaki, S. Asada & K. Fukahara, Recent Research on Cooling Power of Liquid Quenchants, 2nd Int. Conf. on Quenching and the Control of Distortion, 1996, p 37-46.

[11] N.I. Kobasko, Effect of Accuracy of Temperature Measurements on Determination of Heat Transfer Coefficient during Quenching in Liquid Media, J. ASTM Int., Vol. 9 No.2,2012.

[12] R.L. Simencio Otero, Calculation of Kobasko's Simplified HTC from Cooling Curve Data Obtained with Small Probes, J. ASTM Int., Vol. 9, No. 4, 2012

[13] B. Liscic, S. Singer & H. Beitz, Dependence of Heat Transfer Coefficient at Quenching on Diameter of Cylindrical Workpieces, J. ASTM Intl., Vol. 8, No. 7.